HHS Public Access

Author manuscript

J Am Chem Soc. Author manuscript; available in PMC 2019 September 26.

Published in final edited form as:

J Am Chem Soc. 2018 September 26; 140(38): 11926–11930. doi:10.1021/jacs.8b07753.

Reversible Photochemical Control of Protein Localization in Living Cells using a Photocaged-photocleavable Dimerizer

Chanat Aonbangkhen[†], **Huaiying Zhang**[‡], **Daniel Z. Wu**[†], **Michael A. Lampson**[‡], and **David M. Chenoweth**[†]

[†] Department of Chemistry, University of Pennsylvania, 231 South 34th Street, Philadelphia, PA, 19104, USA.

[‡] Department of Biology, University of Pennsylvania, 231 South 34th Street, Philadelphia, PA, 19104, USA.

Abstract

Many dynamic biological processes are regulated by protein-protein interactions and protein localization. Experimental techniques to probe such processes with temporal and spatial precision include photoactivatable proteins and chemically-induced dimerization (CID) of proteins. CID has been used to study several cellular events, especially cell signaling networks, which are often reversible. However, chemical dimerizers that can be both rapidly activated and deactivated with high spatiotemporal resolution are currently limited. Herein, we present a novel chemical inducer of protein dimerization that can be rapidly turned on and off using single pulses of light at two orthogonal wavelengths. We demonstrate the utility of this molecule by controlling peroxisome transport and mitotic checkpoint signaling in living cells. Our system highlights and enhances the spatiotemporal control offered by CID. This tool addresses biological questions on sub-cellular levels by controlling protein-protein interactions.

Graphic entry for the Table of Contents (TOC):

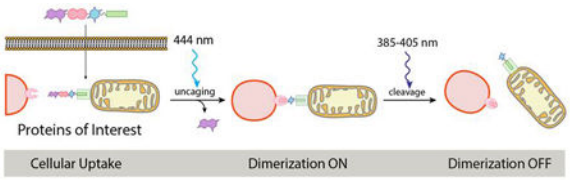

Protein-protein interactions are a fundamental driving force in biological processes, and localization of proteins is one of the mechanisms that cells exploit to regulate numerous biological signaling networks with precise control in time and space. To dissect these complex biological systems, experimental tools that can reversibly manipulate protein localization with comparable precision are necessary. Chemically induced dimerization

Corresponding Authors D.M.C. (dcheno@sas.upenn.edu), M.A.L. (lampson@sas.upenn.edu).

ASSOCIATED CONTENT

Supporting Information. Included are general methods, experimental protocols, synthesis of molecules, and characterization data. This material is available free of charge via the Internet at http://pubs.acs.org.

The authors declare no competing financial interests.

(CID) is a robust and powerful technique that is used to control protein-protein interactions between two proteins that both bind the same small molecule (1–4). However, the lack of spatiotemporal and reversible control of conventional CID have led to the development of new optogenetic systems by introducing light control to the CID technique (5–9). We previously reported a photocaged chemical dimerizer that allows protein recruitment with light to many subcellular locations, such as a single centromere, kinetochore, mitochondrion, and centrosome (10–12). More recently, we introduced a new photocaged dimerizer, which requires less light to be uncaged and is sensitive to longer wavelengths, and a photocleavable dimerizer for which light can be used to reverse dimerization (11–12). However, to study both the gain and loss of function of reversible protein recruitment in the same cell using an optogenetic approach, a dimerizer that can be both activated and deactivated by light is required. To accomplish this goal, we created a novel molecule based on the modular design of our previous dimerizers. Herein, we report a cell-permeable photocaged-photocleavable dimerizer that is capable of turning on and off protein dimerization using two orthogonal wavelengths of light (Figure 1a, b). We show that the dimerizer rapidly induces protein dimerization and dissociation within seconds upon illumination at various locations in the cell, such as mitochondria and plasma membrane. Furthermore, we demonstrate the utility of our new system by controlling peroxisome transport and mitotic checkpoint signaling with high spatiotemporal resolution.

Rational Design Strategy.

The dimerizer CTNH is composed of four sequential modules: a coumarin photocage, a caged trimethoprim (TMP) ligand, a photocleavable nitroveratryl (NV) linker and a non-caged HaloTag ligand (haloligand). TMP is the ligand to *E.coli* dihydrofolate reductase (eDHFR) and the chloroalkane is the ligand for HaloTag protein (haloenzyme). We previously demonstrated that DEACM can be selectively removed with 444-nm light, while NV can be removed by ultraviolet (UV) light up to 405 nm, indicating that these two moieties can potentially be employed for sequential photo-uncaging (10). Moreover, it has been reported that (7-(diethylamino)coumarin-4-yl) methyl (DEACM) has significant photon absorption and high quantum efficiency at 440 nm whereas 3,4-dimethoxy-6-nitrobenzyl or nitroveratryl (NV) exhibits its highest absorption at 365 nm but almost no absorption at >400 nm (13). Evidently, DEACM and NV have also been simultaneously utilized as a pair of photoprotecting groups for selective photo-cleavage of caged phosphoamino acids and caged cAMP- and cGMP in biological systems (14, 15) and for photo-patterning on glass surface (16). In addition, the absorption spectra of DEACM and NV are sufficiently blue-shifted to protect them from undesired cleavage at wavelengths commonly used for imaging (e.g., 488 nm) (Figure S1). Therefore, we selected DEACM (blue moiety in the chemical structure) as a photocage and NV (purple moiety) for incorporation into the linker between the two ligands of the dimerizer (Fig 1a). The dimerizer forms a stable complex with haloenzyme, and illumination with the first wavelength (444 nm) selectively removes the DEACM photocaging group to initiate binding to eDHFR without cleaving the NV linker. Illumination with the second wavelength (387–405 nm) photocleaves the dimerizer to reverse the protein dimerization (Figure 1b). See Supporting Information for detailed rational design strategy.

Rapid light-controlled protein dimerization and reversal at multiple locations in living cells.

To validate our protein dimerization strategy, we initially targeted mitochondria, which are highly dynamic, membrane-bound organelles involved in oxidative metabolism, apoptotic signaling, and other critical cellular pathways (17–18). To test the ability of CTNH to reversibly recruit a freely diffusible protein to mitochondria, we localized haloenzyme to the cytosolic face of the mitochondrial outer membrane by fusing it to the C-terminal domain of the *Listeria monocytogenes* ActA protein. HeLa cells expressing eDHFR fused to mCherry (mCherry–eDHFR) and ActA fused to GFP and haloenzyme (Halo-GFP-Mito) (6) were incubated with 20 μM CTNH for 30 min, followed by a 30-min wash-out. No localization of mCherry to mitochondria was observed prior to illumination, indicating that caging TMP with DEACM completely blocks binding to eDHFR (Figure S6a). Upon illumination with 444-nm light, rapid localization of mCherry-eDHFR was observed at the mitochondria (Figure S6a). The interaction between TMP and eDHFR is not covalent but, in steady state, the localization is persistent (Figure S5a). Upon whole-field illumination with ~387 nm light (Figure S5a) or a targeted 405-nm laser (Figure S6a), mCherry-eDHFR was released from mitochondria, demonstrating that protein dimerization was efficiently reversed by photocleavage of the NV linker with high spatial and temporal control. We next targeted the plasma membrane, an important site for numerous cell signaling pathways (19) where multiple biological phenomena have been studied using CID, including lipid signaling, Ras-regulated pathways, cell protrusion, and migration (20–21). We used HeLa cells expressing cytosolic mCherry-eDHFR and haloenzyme-GFP fused to the CAAX motif, a common plasma membrane targeting sequence. The C-terminus of CAAX proteins undergoes a series of post-translational modifications, resulting in cell membrane localization (23). Global recruitment of cytosolic mCherry-eDHFR was observed at the plasma membrane after 444-nm illumination and rapidly reversed upon 387-nm illumination on a timescale of one second (Figure S5b).

These results highlight the fast kinetics and spatial control of CTNH uncaging and cleavage using light, and show that a variety of subcellular locations, both cytosolic and nuclear, can be targeted to recruit and release a cytosolic protein. We show that CTNH can be widely applicable for rapid and reversible control of protein dimerization at many different subcellular locations. We sought to apply this tool to control more dynamic biological processes.

Reversible control of organelle transport within subcellular regions.

Organelle transport is an essential biological process in eukaryotes and contributes to intracellular organization and cell polarity (24). Various tools have been developed in order to probe functions of organelle positioning (25–26). As a functional test for CTNH, we employed a previously reported peroxisome transport assay in living cells (27–28). Peroxisomes are membrane-bound organelles that play a crucial role in the catabolism of fatty acids, reduction of reactive oxygen species, and biosynthesis of plasmalogens and ether phospholipids (29). Because peroxisomes are immobile under normal steady-state

conditions, movement induced by light is easily observed, providing an ideal assay to test our new dimerizer. To control peroxisome transport, we employed HeLa cells expressing PEX3-GFP-Halo, a peroxisome-targeting sequence fused to GFP-haloenzyme, and KLC1-mCherry-eDHFR, a fusion protein of mCherry-eDHFR linked to kinesin light chain 1 (KLC1) that binds and recruits kinesinheavy chain (Fig. 2a). Prior to illumination, the peroxisomes spread throughout the cell, and KLC1- mCherry-eDHFR diffused in the cytosol (Fig. 2b). After global activation of CTNH with a 444-nm laser, the perox-isomes were initially transported towards the plus ends of the microtubules at the cell periphery. Then, half of the cell was targeted for cleavage of CTNH with a 405-nm laser (Fig. 2b, dashed yellow region). As a result, the induced peroxisome transport was disrupted in this region with no significant change in the peroxisome density after 405-nm illumination and no accumulation of peroxisomes at the cell periphery (Figures 2b-c, regions 1 and 4). In contrast, peroxisome transport continued in the other half of the cell, which was not illuminated with the 405-nm laser, leading to a decrease in GFP intensity over time in the interior of this region and an increase at the periphery (Figs. 2b-c, regions 2 and 3). At the cell periphery, the ratio of the GFP intensity in the uncleaved region to the cleaved region increased significantly after 405-nm illumination, indicating that peroxisomes only accumulated in the uncleaved region (Fig. 2d). Together, these results demonstrate that we can successfully employ light to in-duce and disrupt peroxisome transport with spatiotemporal control.

Activating and silencing the mitotic checkpoint.

To achieve proper chromosome segregation in mitosis, the spindle checkpoint is initially activated until all chromosomes are properly attached to the spindle, and then silenced at metaphase to allow progression to anaphase. For checkpoint signaling proteins, localization to and release from kinetochores are essential steps in checkpoint activation and silencing, respectively, that determine cell fate. With CTNH, we aimed to optically control both steps by manipulating kinetochore localization of the checkpoint protein Mad1 (Fig. 3a). HeLa cells expressing Halo-GFP-SPC25, which localizes to kinetochores, and eDHFR-mCherry-Mad1 (10) were incubated with CTNH. The checkpoint is silenced at metaphase, and >80% of control metaphase cells that were not exposed to 444-nm light proceeded to anaphase normally (Fig. 3b,d). In contrast, after recruiting Mad1 from the cytosol to kinetochores using 444-nm light, <20% of cells proceeded to anaphase within 30 min, demonstrating that the checkpoint can be re-activated with light. To show that the checkpoint can be silenced with light, we recruited Mad1 to kinetochores with 444 nm light and then cleaved CTNH in some cells with a 405-nm laser (Fig. 3c). Without cleavage, Mad1 remained at kinetochores, and <10% of the cells proceeded to anaphase within 30 min, indicating that the mitotic checkpoint remained active. In comparison, >60% of the cells in which Mad1 was released from kinetochores entered anaphase (Figs. 3c,d). This re-activation and silencing of the mitotic checkpoint is consistent with our previous observations using rapamycin (30), which is not sensitive to light, and using a dimerizer that is not caged but can be photocleaved (10). However, with CTNH, both checkpoint activation and silencing can be controlled with light. These results demonstrate that we can use CTNH to manipulate kinetochore function in single cells.

We have developed a novel cell-permeable chemical inducer that can rapidly produce a discrete ON and then OFF state for spatiotemporal control of protein dimerization. Our results highlight the advantages of a hybrid chemical and genetic approach and of our modular design, which facilitates the development of new dimerizers with additional properties tailored for specific purposes. We demonstrate that many subcellular locations, such as plasma membrane, mitochondria, peroxisomes, centromeres and kinetochores, can be targeted with spatial precision for both recruitment and release of a cytosolic protein on a timescale of seconds. We demonstrated that peroxisome transport can be rapidly induced and disrupted on a subcellular length scale. Additionally, we applied this tool to manipulate kinetochore function by controlling mitotic checkpoint signaling. Our future goal is to use this dimerizer in conjunction with other orthogonal dimerizers to control multiple target proteins within a cell. This approach opens up a new avenue for probing a variety of biological processes, such as organelle transport, signal transduction, and cell division. We envision that our new chemical tool will be readily adopted to answer new biological questions that would be otherwise difficult to address with conventional methods.

Supplementary Material

Refer to Web version on PubMed Central for supplementary material.

ACKNOWLEDGMENTS

The JF585 HaloTag ligand was a kind gift from Dr. Luke Lavis (Janelia Research Campus, HHMI). We wish to thank Dr. George Furst and Dr. Jun Gu for NMR assistance, Dr. Rakesh Kohli for high-resolution mass spectrometry (HRMS) assistance, Dr. Evan Smoak, Dr. Abram Calderon and Mr. Alpler Gokden, and Ms. Alyssa Mayo for help with cell culture and microscopy, and the members of the Lampson lab, particularly Dr. Edward R. Ballister for helpful discussions on the project and manuscript, and providing the plasma membrane plasmid. C.A. wishes to thank Dr. Yang Hai and Dr. Mengbin Chen for their help with protein-ligand docking, and Alex Kasznel for helpful discussions on the manuscript. C.A. also wishes to thank the Royal Thai Government for the PhD fellowship funding through the Development and Promotion of Science and Technology (DPST) Project. This work was supported by the National Institutes of Health (GM083988 and GM122475 to M.A.L. and GM118510 to D.M.C.) and the National Institutes of Health, National Cancer Institute (U54-CA193417).

REFERENCES

(1). Stanton BZ; Chory EJ; Crabtree GR Science 2018, 359, eaao5902.

(2). Putyrski M; Schultz C FEBS Lett. 2012, 586, 2097–2105. [PubMed: 22584056]

(3). Fegan A; White B; Carlson JCT; Wagner CR Chem. Rev. 2010, 110, 3315–3336. [PubMed: 20353181]

(4). Derose R; Miyamoto T; Inoue T Pflügers Arch. Eur. J. Physiol. 2013, 465, 409–417. [PubMed: 23299847]

(5). VoB S; Klewer L; Wu YW Curr. Opin. Chem. Biol. 2015, 28, 194–201. [PubMed: 26431673]

(6). Ballister ER; Aonbangkhen C; Mayo AM; Lampson MA; Chenoweth DM Nat. Commun. 2014, 5, 5475. [PubMed: 25400104]

(7). Ankenbruck N; Courtney T; Naro Y; Deiters A An- gew. Chem. Int. Ed. 2018, 56, 2768–2798.

(8). Brown K; Zou Y; Zhang J; Shirvanyants D; Samanta S; Mantravadi P; Dokholyan NV; Deiters A Chem. Commun. 2015, 51, 5702–5705.

(9). Caldwell RM; Bermudez JG; Thai D; Aonbangkhen C; Schuster BS; Courtney T; Deiters A; Hammer DA; Chenoweth DM; Good MC Biochemistry 2018, 57, 2590–2596. [PubMed: 29671583]

(10). Zhang H, Aonbangkhen C Tarasovetc EV, Ballister ER, Chenoweth DM, Lampson MA Optogenetic control of kinetochore function. Nat. Chem. Biol. 2017, 13, 1096–1101. [PubMed: 28805800]

(11). Zhang H; Chenoweth DM; Lampson MA Mitosis and Meiosis Part A; Elsevier, 2018, 144, 157–164

(12). Akera T; Chmatal L; Trimm E; Yang K; Aonbangkhen C; Chenoweth DM; Janke C; Schultz RM; Lampson MA Science 2017, 358, 668–672. [PubMed: 29097549]

(13). Klan P; Solomek T; Bochet CG; Blanc A; Givens R; Rubina M; Popik V Kostikov A; Wirz J Chem. Rev. 2013, 113, 119–191 [PubMed: 23256727]

(14). Goguen BN; Aemissegger A; Imperiali BJ Am. Chem. Soc. 2011, 33, 11038–11041

(15). Priestman MA; Sun L Lawrence DS ACS Chem. Biol. 2011, 6, 377–384 [PubMed: 21218856]

(16). Stegmaier P; Alonso JM; Campo A Langmuir, 2008, 24, 11872–11879 [PubMed: 18817427]

(17). Friedman JR; Nunnari J Nature 2014, 505, 335–343. [PubMed: 24429632]

(18). Detmer SA; Chan DC Nat. Rev. Mol. Cell Biol. 2007, 8, 870–879. [PubMed: 17928812]

(19). Stone MB; Shelby SA; Veatch SL; Chem. Rev. 2017, 117, 11, 7457–7477. [PubMed: 28211677]

(20). Kim AK; DeRose R; Ueno T; Lin B; Komatsu T; Nakamura H; Inoue T Sci. Signaling. 2016, 9, 414.

(21). Lin B; Yin T; Wu YI; Inoue T; Levchenko A Nat. Commun. 2015, 6, 6619. [PubMed: 25851023]

(22). Feng S; Laketa V; Stein F; Rutkowska A; MacNamara A; Depner S; Klingmüller U; Saez-Rodriguez J; Schultz C Angew. Chemie - Int. Ed. 2014, 53, 6720–6723.

(23). Manolaridis I; Kulkarni K; Dodd RB; Ogasawara S; Zhang Z; Bineva G; O'Reilly N; Hanrahan SJ; Thompson AJ; Cronin N; Iwata S; Barford D Nature. 2013, 504, 301–305. [PubMed: 24291792]

(24). Bornens M Nat. Rev. Mol. Cell. Biol. 2008, 9, 874–886. [PubMed: 18946476]

(25). van Bergeijk P; Hoogenraad CC; Kapitein LC Trends Cell Biol. 2016, 26, 121–134. [PubMed: 26541125]

(26). van Bergeijk P; Adrian M; Hoogenraad CC; Kapitein LC Nature. 2015, 518, 111–4. [PubMed: 25561173]

(27). Kapitein LC; Schlager MA; van der Zwan WA; Wulf PS; Keijzer N; Hoogenraad CC Biophys. J. 2010, 99, 2143–2152. [PubMed: 20923648]

(28). Ballister ER; Ayloo S; Chenoweth DM; Lampson MA; Holzbaur ELF Curr. Biol. 2015, 25, R407–8. [PubMed: 25989077]

(29). Smith JJ; Aitchison JD Nat. Rev. Mol. Cell Biol. 2013, 14, 803–817. [PubMed: 24263361]

(30). Ballister ER; Riegman M; Lampson MA J. Cell Biol. 2014, 204, 901–908. [PubMed: 24637323]

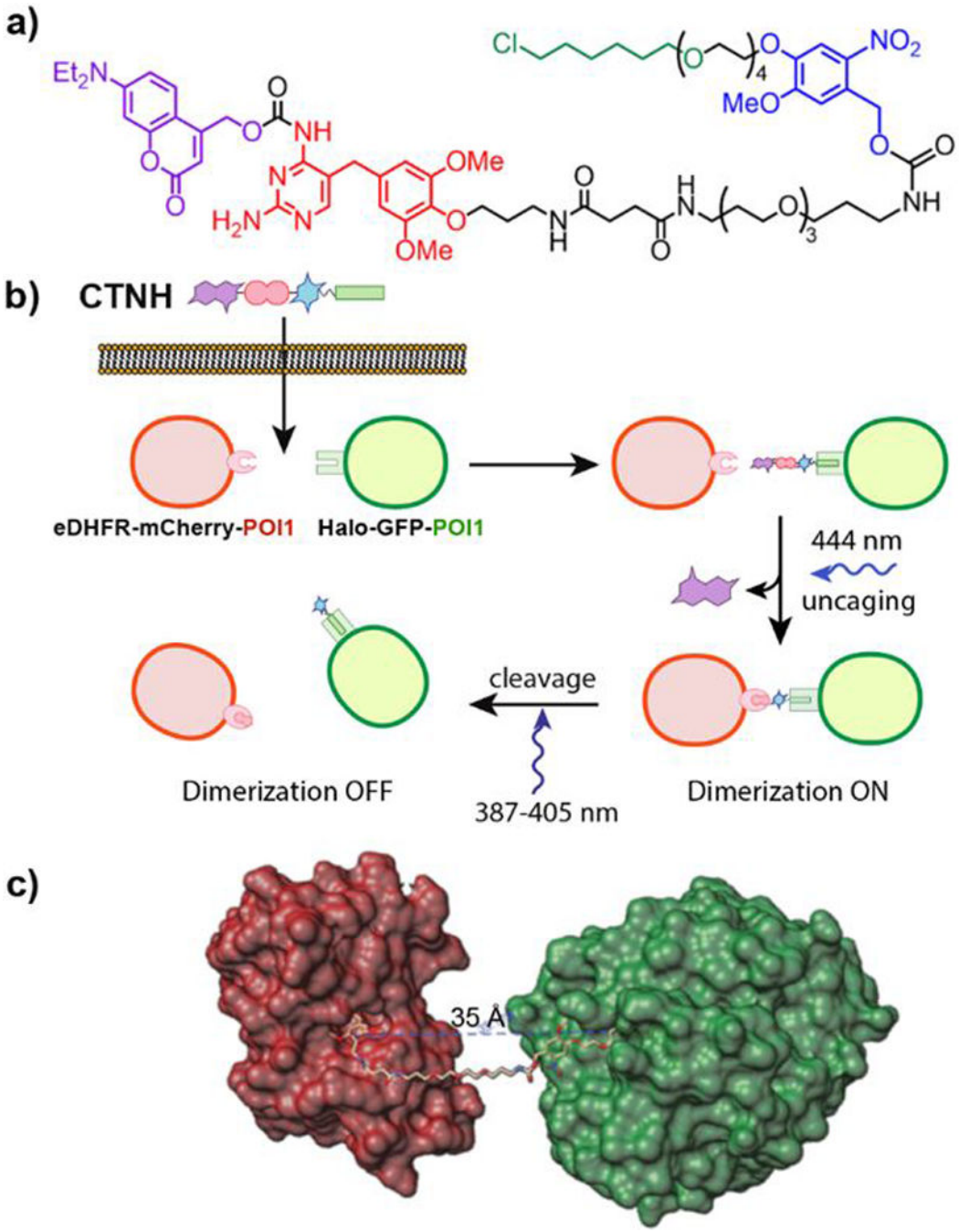

Figure 1. Light-induced protein dimerization and reversal with CTNH.

(a) Chemical structure of CTNH. (b) Two different wavelengths of light were employed to uncage and cleave CTNH to induce protein dimerization and reversal of protein dimerization. (c) Model of protein complex dimerized by CTNH that was obtained by superimposition of the CTNH dimerizer to trimethoprim (TMP) and haloligand complexed with eDHFR (PDB: 1RG7) and haloenzyme (PDB: 1BN7), respectively.

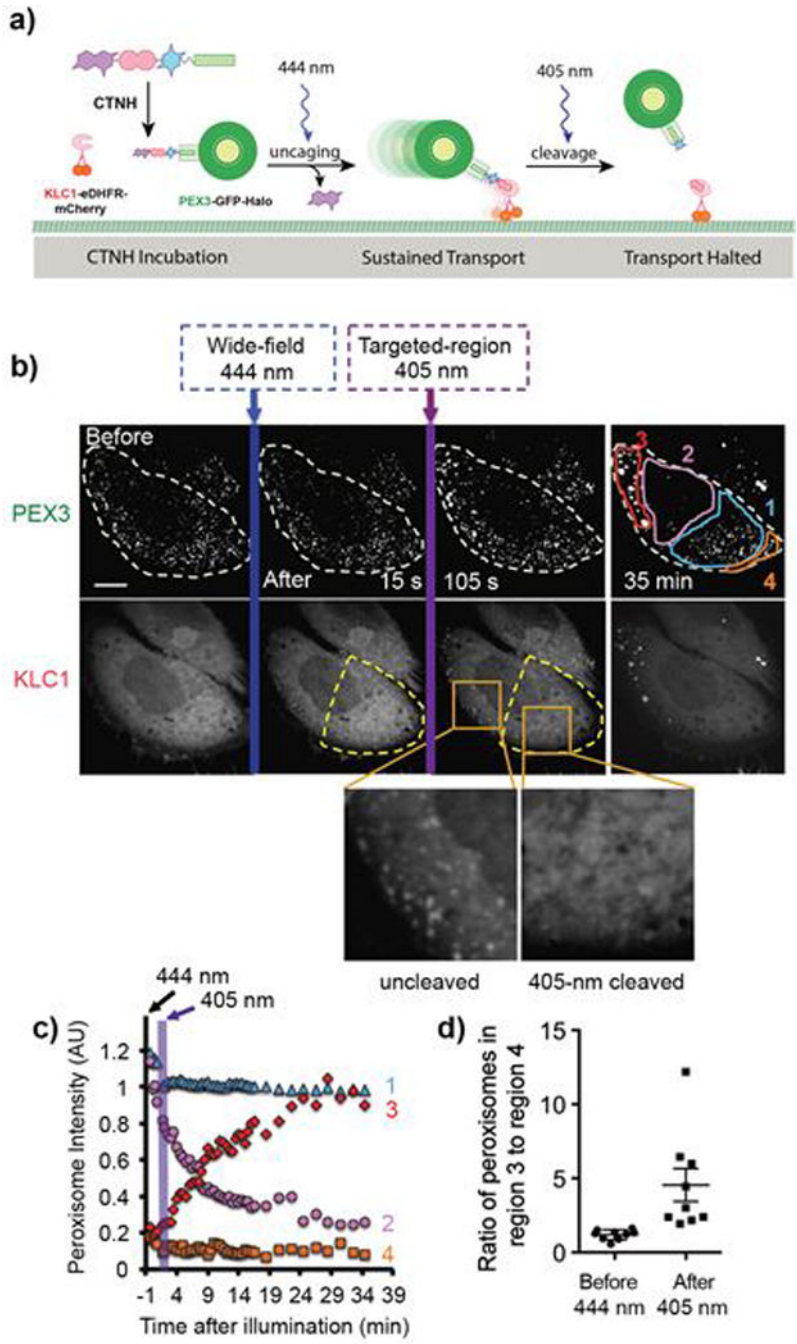

Figure 2. Controlling peroxisome transport with light.

(a) Schematic and protein constructs. (b-d) HeLa cells expressing PEX3-GFP-Halo and KLC1-mCherry-eDHFR incubated with 20 μM CTNH followed by washout. CTNH was uncaged with 444-nm light at t = 0 to recruit KLC1-mCherry-eDHFR to peroxisomes. In a representative cell (b), dashed white and yellow lines indicate the cell outline and the photocleaved area, respectively, and orange square insets show KLC1 release from peroxisomes in the cleaved area. GFP intensity was quantified (c) in interior and peripheral regions in both the cleaved (regions 1 and 4) and uncleaved (regions 2 and 3) areas. Intensity

in each region over time is shown as a fraction of the maximal intensity observed in that region. The average GFP intensity (as a proxy for peroxisome density) at the cell periphery was quantified (d) as a ratio of region 3 to region 4, both before uncaging with 444-nm light and after cleavage with 405-nm laser at the final timepoint (t = 35 min). Each dot represents an individual cell and the mean±sem is shown (n = 9 cells pooled from three independent experiments). ***P < 0.005, paired Student's t-test. Scale bars, 10 μm.

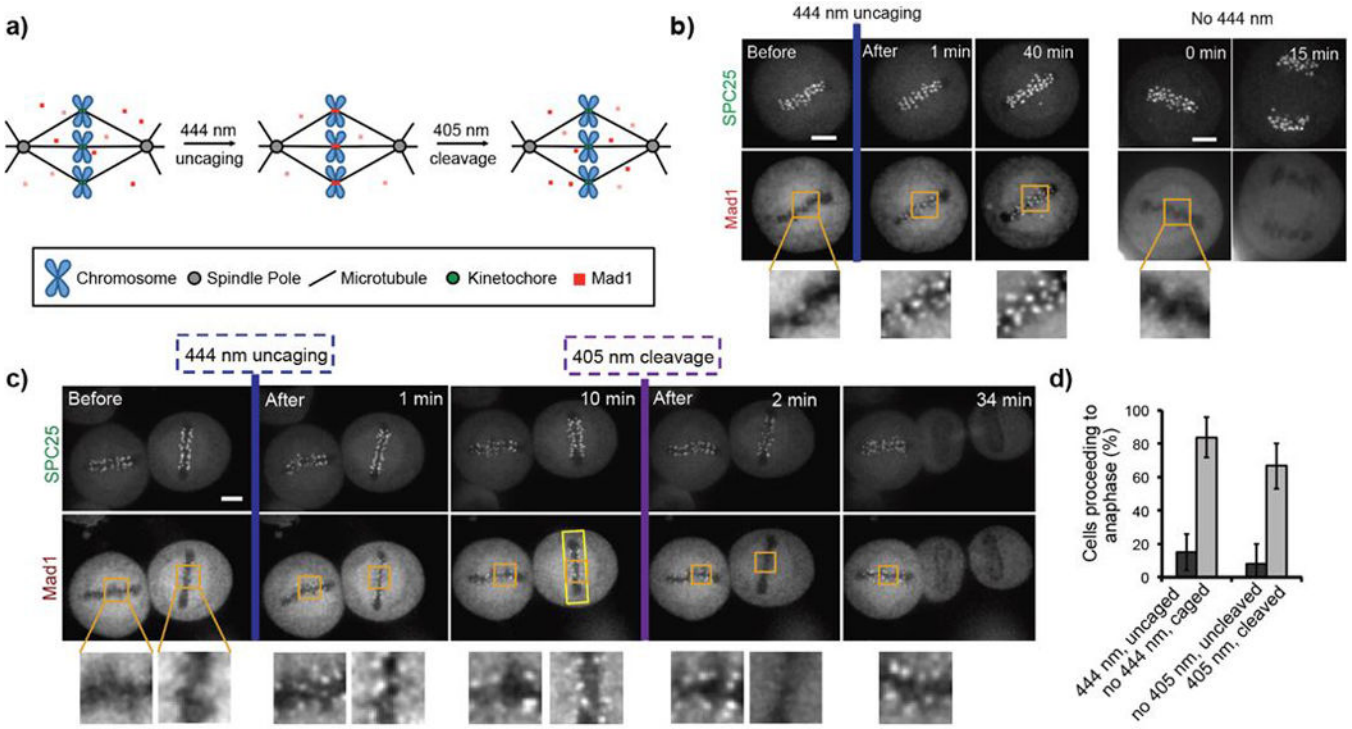

Figure 3. Activating and silencing the spindle assembly checkpoint.

(a) Experimental design using CTNH for light-induced recruitment of Mad1 to and release from kinetochores. (b-d) HeLa cells expressing Halo-GFP-SPC25 and mCherry-eDHFR-Mad1 were incubated with 10 μM CTNH followed by washout. (b) Upon illumination with 444-nm light in some cells, Mad1 was recruited to metaphase kinetochores and cells arrested in metaphase (left panel). Cells without Mad1 recruitment to metaphase kinetochores proceeded to anaphase normally (right panel). Brown square insets show magnified regions in mCherry channel. (c) After global illumination with 444-nm light, Mad1 was released from kinetochores in some cells using a 405-nm laser to target the metaphase plate (c, right cell, yellow region), while other cells were not exposed to 405-nm light. Orange square insets show magnified regions in mCherry channel. (d) The percentage of cells entering anaphase within ~30 minutes after 444-nm uncaging in (b) and after 405-nm photocleavage in (c) was quantified for both cell populations. Error bars represent s.d. (number of cells in each condition, n = 15 for uncaged; n = 21 for caged; n = 20 for uncleaved; n = 25 for cleaved population, pooled from three independent experiments). Scale bars, 5 μm